

Technological aspects of solid oxide fuel cells with scandia-stabilized zirconia electrolyte

M. I. Lugovy, V. M. Slyunyayev, M. P. Brodnikovskyy

It is the aim of the present work to address some of the aspects of optimized technological approach of manufacturing planar anode-bearing solid oxide fuel cells based on detailed investigation of such effects as electrolyte microcracking and degradation, taking into account weakening of its grain boundaries due to impurity segregation during SOFC operation. The combination of electron microscopy research with model calculations permits both the specific energy of new surface creation in the electrolyte and critical parameters of the microcracking process to be determined. The accounting of segregation behavior features allows one to control electrolyte brittleness by using of optimal heat treatment regimes.

Keywords: *solid oxide fuel cell, electrolyte, microcracking, grain boundary, impurity.*

Introduction

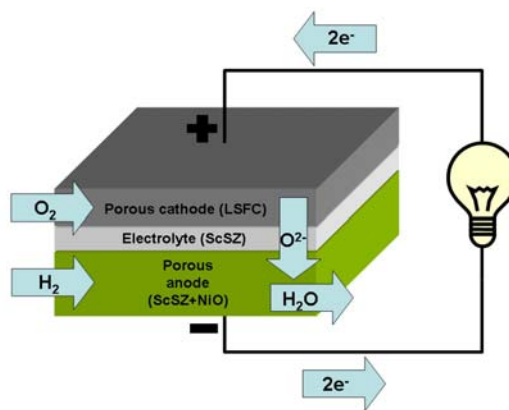
Promising options for future energy supply are offered by solid oxide fuel cells (SOFC) due to the high electrical energy conversion efficiency they display. The applications of SOFC are ranged from centralised MW scale generation through to localised applications at 100+ kW level for distributed generation to local domestic generation on the 1 to 10 kW scale. Wide range of other applications such as corrosion protection, uninterruptible power supply, remote generation, and domestic appliances is also required. Commercialisation of these applications will require even lower operating temperatures and additional material improvements [1].

An air electrode (cathode), electrolyte, and a fuel electrode (anode) are main constituents of a single SOFC [2] (fig. 1). The transport of oxide ions from the electrolyte's interface with the air electrode to its interface with the fuel electrode is the function of the electrolyte. The function of the cathode is to facilitate the reduction of oxygen molecules to oxide ions transporting electrons to the electrode/electrolyte interface to allow gas diffusion to and from this interface. The function of the anode is to facilitate the oxidation of the fuel and the transport of electrons from the electrolyte to the fuel electrode interface. In addition the anode must allow diffusion of fuel gas to and exhaust gases away from this interface.

Still, several major problems remain to be solved: degradation is too high (between 0,5 and 2% per 1000 hours of operation, resulting in a 'lifetime' of around 10 000 to 30 000 operating hours); costs are too high (above 10 000 Euro/kW); intermittent operation (thermal and oxidation cycling) results in increased degradation and/or failure; power density at temperatures below 1023 K is comparatively low [3]. These problems are a consequence of the high temperatures, elevated pressures required for their operation, and the ceramics materials properties [4].

High ion conductivity of scandia-stabilised-zirconia-based electrolyte offers the potential for lowering the SOFC's operating temperature with an ensuing

Fig. 1. Planar solid oxide fuel cell with ScSZ electrolyte.



reduction of corrosion and degradation effects. SOFC operating between 873 and 1073 K are generally labelled “intermediate temperature” SOFC (IT-SOFC). In addition, the higher conductivity can also be considered as a potential for obtaining very much higher power densities at operating temperatures above 1023 K. Using thin electrolyte membranes with thicknesses between 5 and 50 μm is another way of minimizing ohmic losses across the electrolyte. A promising technique to produce thin films of electrolyte on thick anode substrates of planar geometry is electron beam deposition (EBD). The anode supported planar SOFC cell has become one of the most widespread SOFC types.

A challenge with the planar geometries is in obtaining mechanically stable structures, as thin layer ceramics are inherently susceptible to failure when subjected to moderate stress. If the anode is produced from a nickel oxide — ScSZ composite and the electrolyte from scandia-stabilised zirconia, thermal mismatch stresses keep the electrolyte layer under compression at room temperature and under tension at temperatures higher than the deposition temperature. The mechanical properties of the SOFC components, including the electrolyte, must be known in order to design an optimal SOFC structure. Typically, the electrolyte shows microcracking due to residual stress [5].

The goal of the work is to develop an optimized technological approach of manufacturing planar anode-bearing solid oxide fuel cells based on detailed investigation of such effects as electrolyte microcracking and degradation, taking into account weakening of its grain boundaries due to impurity segregation during SOFC operation. The importance of such research is related to the fact that SOFC’s mechanical integrity is a condition of its reliability during long-term exploitation.

Experimental

The composition 10% (mol.) Sc_2O_3 — 1% (mol.) CeO_2 — 89% (mol.) ZrO_2 (10Sc1CeSZ) was found to be optimal for the electrolyte and as a constituent of the anode [6]. SOFC anodes were fabricated with a traditional ceramic route. Mixtures of 40% (wt.) NiO and 60% (wt.) 10Sc1CeSZ were ball-milled with alcohol for 24 hours. Polyvinyl alcohol was used as pore-creating agent. Specimens were made by uniaxial pressing using pressure ~ 20 MPa. These were sintered at 1723 K for 2 hours in air. The anode substrates were found to meet all necessary requirements concerning both strength and porosity (100—150 MPa and 25—30%, respectively). The thickness of the anodes was 990 μm .

$\text{La}_{0.8}\text{Sr}_{0.2}\text{Co}_{0.8}\text{Fe}_{0.2}\text{O}_3$ (LSCF) cathode material was prepared by conventional solid-state reaction, using powders of La_2O_3 , SrO, CoO and Fe_2O_3 (all 99% purity provided by Miranda-C). The ceramic route was done by ball-milling stoichiometric quantities of the reagents with ethanol for 24 hours.

The resulted mixture was dried and calcinated in air at 900 °C for 4 hours in order to develop the perovskite phase and ground again.

EBD technique was used for producing electrolyte films deposited on the porous, non-reduced anode substrates. Hereafter the electrolyte — anode layered system will be termed “half-cell”. “Half-cell” is a necessary intermediate step of producing full fuel cell. EBD is one form of physical vapor deposition (PVD). An electron beam is directed at a target pellet, in order to ionize and melt the target material, which is then accelerated in an electrical field and deposits on the specimen to be coated. The process is rather slow but results in a very precise control of layer thickness and, when applied expertly, delivers very thin, dense coatings, as needed for intermediate temperature electrolytes [7]. These thin layers again reduce the overall resistance of the electrolyte and further support the trend towards higher power density/lower operating temperatures. Powder metallurgy routes were applied to produce ScSZ specimens to be used for further electron-beam deposition experiments. The dimensions of the cylindrically shaped specimens were about 4 mm in diameter and about 8 mm in height (porosity approx. 15%). The substrates were subjected to temperatures of 873, 1023 and 1173 K (deposition temperature) during the deposition process. The deposition time of 15 min resulted in the formation of electrolyte films with 10 µm in thickness.

Standard techniques, scanning electron microscopy and Image-Pro Plus Software (Version 3.0.00.00, “Media Cybernetics”), were applied to obtain electrolyte microstructure images and to evaluate microcrack sizes as well as the number of microcracks in the electrolyte layer. Using Image-Pro Plus Software for all considered states of electrolyte, the length of each microcrack observed in corresponding image was measured. The microcrack density was calculated as:

$$f_f = \frac{1}{A} \sum_{i=1}^{N_A} c_i^2, \quad (1)$$

where c_i is the effective length of the i -th microcrack, and N_A is the number of microcracks on the scanned area A (in our case $A = 45000 \mu\text{m}^2$).

Results and discussion

It is of top interest to know mechanical properties of EBD 10Sc1CeSZ electrolyte in order to optimize fuel cell processing. One of the possible approaches to characterize the mechanical properties of EBD electrolyte films is to use heat treatment of half-cells, i. e. annealing at various temperatures above deposition temperature followed by electron microscopy investigation of the electrolyte surface. The annealing creates equibiaxial stress states with tensile stress in the electrolyte, whose value depends on the difference ΔT between annealing temperature and deposition temperature [5]. Electron microscopy investigations of the electrolyte surface have allowed the density of microcracks arising due to tensile residual stresses in the annealed electrolyte to be determined (fig. 2).

The initial data for thermal stress calculation in half-cells were established experimentally and via literature survey. The elastic modulus for the anode material was found to be 81 GPa from four point bending tests. The elastic modulus of an undamaged electrolyte was adopted to be 200 GPa [8]. It is

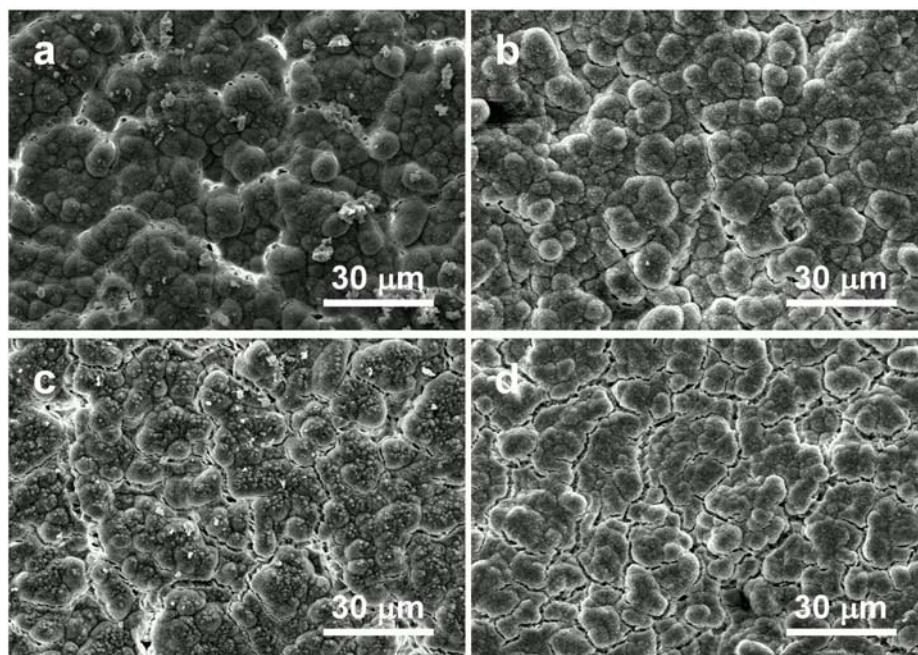


Fig. 2. Microstructure of EBD 10Sc1 CeSZ electrolyte film after deposition and annealing: *a* — deposition at 1173 K, annealing at 1473 K; *b* — deposition at 873 K, annealing at 1178 K; *c* — deposition at 1023 K, annealing at 1473 K; *d* — deposition at 873 K, annealing at 1473 K.

known that the elastic modulus of ceramics as a rule demonstrates a dependence on temperature. For example, the existence of such dependence for yttria-stabilized zirconia (YSZ) is shown in [9] where a substantial scattering of experimental data is observed. The scattering complicates the determination of a reliable dependence of elastic modulus on temperature. To the best of our knowledge, the temperature dependence of the elastic modulus for 10Sc1CeSZ is not available from literature. Therefore, as a first approximation, a constant value of the elastic modulus is used for calculation in this work. The Poisson ratios of anode and electrolyte were adopted to be 0,3 and 0,31, respectively [9]. The coefficient of thermal expansion for the anode was found experimentally to be $11,7 \cdot 10^{-6} \text{ K}^{-1}$. The coefficient of thermal expansion for the electrolyte was adopted to be $1 \cdot 10^{-5} \text{ K}^{-1}$ [10]. Note that non-reduced anode substrate was used in this work. In such a way, there are not particles of pure nickel in the anode. This means that creep processes in the anode during annealing were negligible, simplifying residual stress calculation.

It is found that the microcrack density is negligible at $\Delta T = 150 \text{ K}$ demonstrating the practical absence of microcracking due to stresses associated with this temperature difference. Increasing the temperature difference gives rise to a growth of the microcrack density which promotes the significant decrease of the electrolyte elastic modulus and Poisson ratio [11]. In turn, this results in decreasing effective thermal stresses in the electrolyte. The effective elastic properties of the electrolyte (Young modulus E , Poisson ratio ν) and acting thermal stresses σ corresponding to different ΔT are listed in table. The dependence of the tensile stresses on microcrack density can be compared with the model calculations made in [5].

The effective elastic properties of 10Sc1CeSZ electrolyte film and thermal stresses corresponding to different ΔT

ΔT , K	f_f	E , GPa	ν	σ , MPa
150	0,039	194	0,30	60,6
300	0,392	147	0,23	85,6
305	0,473	138	0,21	80,6
375	1,358	69	0,11	45,0
450	2,103	38	0,06	28,9
460	2,414	30	0,05	23,0
600	3,365	14	0,02	13,9

Note that the combination of experimental observations of microcrack density at different annealing temperatures with model calculations [5, 11—15] allows the critical parameters of electrolyte failure, such as maximum strain energy density and strain energy density corresponding to microcracking initiation, as well as the corresponding stresses to be determined. The parameter necessary for model calculations but unknown at this stage is the specific energy of new surface creation γ . An attempt was made to determine this parameter for the electrolyte material analyzing the experimental data. The lower boundary γ_l and upper boundary γ_u of parameter γ were found to equal 0,035 and 0,037 J/m², respectively [5]. This means the best estimation of the specific energy of new surface creation (with accuracy of 3%) is $\gamma = 0,036$ J/m².

The question arises to what measure the obtained value of the specific energy of new surface creation is realistic and how it compares with literature data. It is shown earlier that the value of the specific energy of new surface creation (0,036 J/m²) for 10Sc1CeSZ electrolyte is reduced essentially in comparison with specific surface energy values of zirconia-based ceramics given in literature [5]. The main reason of the reduction in our opinion can be attributed to the intercrystalline fracture mode of electrolyte film. The energy of intergranular fracture of polycrystalline materials is known to be decreased to some extent compared to the energy of transcrystalline fracture. The decrease is widely considered to be associated with the occurrence of impurity atoms and their segregation to grain boundaries. The segregation is known to affect both mechanical properties and conductivity of ceramics [16—19]. In addition to this possible impurity effect, in our opinion, a second reason for the low specific energy of new surface creation of electrolyte film cannot be ruled out. This is associated with an intrinsic weakness of grain boundaries of the electrolyte film resulting from EBD processing and from its columnar structure. Considering above arguments, it is evident that the energy of free surfaces formed upon intercrystalline brittle failure should be used in our model calculations instead of the surface energy.

The critical parameters of electrolyte microcracking were calculated using the model developed in [5]. The strain energy density corresponding to microcracking initiation and maximum strain energy density were established to be 0,017 MPa and 0,027 MPa, respectively. The stress which corresponds to microcracking initiation, maximum stress and stress corresponding to localised microcracking initiation were found to be 82, 100 and 95 MPa, respectively. The microcrack density corresponding to maximum stress and to localised microcracking initiation were found to equal 0,077 and 0,226, respectively.

The values for the temperature difference ΔT corresponding to microcracking initiation, the maximum stress and the maximum strain energy density were found taking into account the above critical parameters. The temperature differences are 195, 257 and 283 K, respectively. The temperature differences used in this work were 150, 300, 305, 375, 450, 460, and 600 K. Therefore, it is evident that the temperature difference of 150 K has not caused any microcracking, while temperature differences of 300, 305, 375, 450, 460, and 600 K were more than 283 K, thus corresponding to localised microcracking. Note also that the experimental determination of microcrack density in the electrolyte in conditions being within the range from microcrack initiation to maximum stress is a complicated task due to the fact that the corresponding microcrack densities are not far from the so-called background value which is observed in practically non-cracked material. Thus, it is realistic for scattered microcracking to reveal the conditions after maximum stress, i.e., being within the range from maximum stress to maximum strain energy density. In our case this is the range of temperature difference from 257 to 283 K which is a narrow temperature interval of 26 K only. Accounting also for the occurrence of statistical deviations in the microstructure of the electrolyte film, it is a difficult task to fit the annealing conditions into the temperature range of distinct scattered microcracking.

It is known that the small value of parameter γ resulting in intercrystalline fracture of electrolyte is mainly associated with the occurrence of impurity atoms and their segregation to grain boundaries. It was shown earlier [20, 21] two main kinetic factors (impossibility to reach the equilibrium segregation level in conditions of finite time of exposure as well as segregation increment through cooling) result in the non-monotonous temperature dependence of segregation in polycrystalline materials. The accounting of non-monotonous temperature dependence of segregation allows temperature ranges in which susceptibility of electrolyte material to intergranular brittleness increases to be predicted. One of ways to use the approach is to calculate “time-temperature” diagrams of material brittleness. Finally, it allows controlling electrolyte brittleness by using of optimal heat treatment regimes.

Conclusions

The results obtained can be summarized as follows. The combination of electron microscopy data with model calculations permits both the specific energy of new surface creation of the electrolyte and critical parameters of the microcracking process to be determined. The best estimation of the specific energy of new surface creation (with an accuracy of 3%) is $\gamma = 0,036 \text{ J/m}^2$. The strain energy density of microcracking initiation and maximal strain energy density are 0,017 and 0,027 MPa, respectively. The mechanical stress corresponding to microcracking initiation is 82 MPa; the maximum mechanical stress is 100 MPa; the mechanical stress corresponding to initiation of localised microcracking is 95 MPa. The microcrack densities which correspond to maximal stress and to the initiation of localised microcracking are 0,077 and 0,226, respectively. The annealing-induced electrolyte microcracking described here corresponds to localised microcracking, when each next structural element fails mainly at existing microcrack tips. Detailed characterization of electrolyte microcracking is a key issue of SOFC design to prevent electrolyte leaking.

The occurrence of impurity atoms and their segregation to grain boundaries results in the small value of the specific energy of new surface creation and in intercrystalline fracture of electrolyte. The accounting of non-monotonous temperature dependence of segregation allows one to control electrolyte brittleness by using of optimal heat treatment regimes.

1. *Singhal S. C.* Solid oxide fuel cells for stationary, mobile, and military applications // *Solid State Ionics*. — 2002. — **152—153**. — P. 405—410.
2. *Minh N. Q.* Ceramic fuel cells // *J. Amer. Ceram. Soc.* — 1993. — **76**, No. 3. — P. 563—588.
3. *Blum L., Buchkremer H.-P., Gross S. M. et al.* Overview of the development of solid oxide fuel cells at Forschungszentrum Juelich // *Int. J. Appl. Ceram. Technol.* — 2006. — **3**, No. 6. — P. 470—476.
4. *Ralph J. M., Schoeler A. C., Krumpelt M.* Materials for lower temperature solid oxide fuel cells // *J. Mater. Sci.* — 2001. — **36**. — P. 1161—1172.
5. *Lugovy M., Slyunyayev V., Steinberger-Wilckens R.* Microcracking in electron beam deposited scandia-stabilised zirconia electrolyte // *J. Power Sources*. — 2009. — **194**. — P. 950—960.
6. *Yarmolenko S., Sankar J., Bernier N. et al.* Phase stability and sintering behavior of 10% (mol.) Sc_2O_3 —1% (mol.) CeO_2 — ZrO_2 ceramics // *J. Fuel Cell Science and Technology*. — 2009. — **6**. — P. 021007.
7. *Grechanyuk N. I., Osokin V. A., Shpak P. A., Piyuk E. L.* Effect of production parameters on the structure of the outer ceramic layer in two-layer metal–ceramic coatings prepared by electron-beam deposition in one production cycle // *Powder Metall. Met. Ceram.* — 2005. — **44**, No. 3—4. — P. 137—142.
8. *Srikanth V. T., Turner K. T., Ie T. Y. A., Spearing S. M.* Structural design considerations for micro-machined solid-oxide fuel cells // *J. Power Sources*. — 2004. — **125**. — P. 62—69.
9. *Giraud S., Canel J.* Young's modulus of some SOFC materials as a function of temperature // *J. Eur. Ceram. Soc.* — 2008. — **28**. — P. 77—83.
10. *Corbin S. F., Qiao X.* Development of solid oxide fuel cell anodes using metal-coated pore-forming agents // *J. Amer. Ceram. Soc.* — 2003. — **86**, No. 3. — P. 401—406.
11. *Salganik R. L.* Mechanics of solids with large number of cracks // *Izv. AN SSSR (Mekhanika Tverdogo Tela)*. — 1973. — No. 4. — P. 149—158 (in Russian).
12. *Lugovy M., Slyunyayev V., Orlovskaya N. et al.* Apparent fracture toughness of Si_3N_4 -based laminates with residual compressive or tensile stresses in surface layers // *Acta Mater.* — 2005. — **53**. — P. 289—296.
13. *Lugovy M., Slyunyayev V., Teixeira V.* Residual stress relaxation processes in thermal barrier coatings under tension at high temperature // *Surf. Coat. Technol.* — 2004. — **184**. — P. 331—337.
14. *Podrezov Y. N., Lugovoy N. I., Slyunyaev V. N., Minakov N. V.* Statistical failure model of materials with micro-inhomogeneity // *Theor. Appl. Fract. Mech.* — 1997. — **26**. — P. 35—40.
15. *Lugovy M., Slyunyayev V., Subbotin V. et al.* Crack arrest in Si_3N_4 -based layered composites with residual stress // *Compos. Sci. Technol.* — 2004. — **64**. — P. 1947—1957.
16. *Hui S.(R.), Roller J., Yick S. et al.* A brief review of the ionic conductivity enhancement for selected oxide electrolytes // *J. Power Sources*. — 2007. — **172**. — P. 493—502.
17. *Badwal S. P. S., Ciacchi F. T., Giampietro K. M.* Analysis of the conductivity of commercial easy sintering grade 3% (mol.) Y_2O_3 — ZrO_2 materials // *Solid State Ionics*. — 2005. — **176**. — P. 169—178.

18. Wakai F., Nagano T., Iga T. Hardening in creep of alumina by zirconium segregation at the grain boundary // J. Amer. Ceram. Soc. — 1997. — **80**, No. 9. — P. 2361—2366.
19. Ikuhara Y., Yoshida H., Sakuma T. Impurity effects on grain boundary strength in structural ceramics // Mater. Sci. Eng. A. — 2001. — **319—321**. — P. 24—30.
20. Lugovy M. I., Slyunyayev V. M., Brodnikovs'kyi Y. M. et al. Ceramic fuel cells for space vehicles // Space Science and Technology. — 2009. — **15**, No. 2. — P. 5—15 (in Ukrainian).
21. Slyunyayev V. M., Lugovy M. I., Firstov S. A. Grain boundary segregation in a binary alloy upon heat treatment: non-monotonous temperature dependence and effect on intergranular brittleness // Metallofiz. Noveishie Tekhnol. — 2007. — **29**, No. 4. — P. 451—469 (in Russian).

Технологічні засади виробництва паливних комірок з електролітом на базі оксиду цирконію з добавками оксиду скандію

М. І. Луговий, В. М. Слюняєв, М. П. Бродніковський

Розглядаються технологічні засади оптимізації виробництва плоских твердооксидних паливних комірок з несучим анодом на базі оксиду цирконію з добавками оксиду скандію. Наведено результати дослідження мікророзтріскування електроліту згаданого складу, що напилений електронно-променевим способом. При цьому береться до уваги ефект послаблення границь зерен внаслідок виникнення сегрегації домішкових атомів. Питома енергія створення нових поверхонь в електроліті та критичні параметри процесу його мікророзтріскування були визначені за допомогою комбінації електронно-мікроскопічних досліджень з модельними розрахунками. Врахування особливостей поведінки зернограничної сегрегації домішок дозволяє керувати крихкістю електроліту за допомогою використання оптимальних режимів термічної обробки.

Ключові слова: твердооксидні паливні комірки, електроліт, мікророзтріскування, границя зерна, домішки.

Технологические основы разработки топливных элементов с электролитом на основе оксида циркония с добавками оксида скандия

Н. И. Луговой, В. Н. Слюняев, Н. П. Бродниковский

Рассматриваются технологические основы разработки плоских твердооксидных топливных элементов с несущим анодом на основе диоксида циркония, стабилизированного оксидом скандия. Приведены результаты микрорастрескивания электролита, полученного электронно-лучевым напылением. При этом принимается во внимание эффект ослабления границ зерен вследствие сегрегации примесных атомов. С использованием комбинации электронной микроскопии с модельными расчетами определены удельная энергия образования новой поверхности в электролите и критические параметры его микрорастрескивания. Учет особенностей поведения зернограничной сегрегации примесей позволяет контролировать степень хрупкости электролита путем оптимизации режимов термической обработки.

Ключевые слова: твердооксидные топливные элементы, электролит, микрорастрескивание, граница зерна, примесь.